

Caspase-9 Holoenzyme Is a Specific and Optimal Procaspase-3 Processing Machine

Qian Yin,^{1,2} Hyun Ho Park,^{1,3} Jee Y. Chung,^{1,5} Su-Chang Lin,¹ Yu-Chih Lo,¹ Li S. da Graca,⁴ Xuejun Jiang,⁴ and Hao Wu^{1,2,3,*}

¹Department of Biochemistry

²Tri-institutional Training Program in Chemical Biology and

³Graduate School of Medical Sciences

Weill Medical College of Cornell University

⁴Cell Biology Program

Memorial Sloan-Kettering Cancer Center

New York, New York 10021

Summary

Caspase-9 activation is critical for intrinsic cell death. The activity of caspase-9 is increased dramatically upon association with the apoptosome, and the apoptosome bound caspase-9 is the caspase-9 holoenzyme (C9Holo). In this study, we use quantitative enzymatic assays to fully characterize C9Holo and a leucine-zipper-linked dimeric caspase-9 (LZ-C9). We surprisingly show that LZ-C9 is more active than C9Holo for the optimal caspase-9 peptide substrate LEHD-AFC but is much less active than C9Holo for the physiological substrate procaspase-3. The measured K_m values of C9Holo and LZ-C9 for LEHD-AFC are similar, demonstrating that dimerization is sufficient for catalytic activation of caspase-9. The lower activity of C9Holo against LEHD-AFC may be attributed to incomplete C9Holo assembly. However, the measured K_m of C9Holo for procaspase-3 is much lower than that of LZ-C9. Therefore, in addition to dimerization, the apoptosome activates caspase-9 by enhancing its affinity for procaspase-3, which is important for procaspase-3 activation at the physiological concentration.

Introduction

Caspase activation is a hallmark of apoptotic cell death (Riedl and Shi, 2004; Salvesen, 2002). According to their sequence of activation, caspases may be divided into two groups: initiator caspases such as caspase-8, -9, and -10, and effector caspases such as caspase-3 and -7 (Salvesen, 2002; Shi, 2002). In the classical paradigm of apoptosis, there are two general pathways for caspase activation and apoptosis induction (Danial and Korsmeyer, 2004). In the extrinsic apoptosis pathway, death ligands interact with and activate death receptors, leading to the assembly of the death-inducing signaling complex (DISC) that activates caspase-8 and caspase-10. In the intrinsic apoptotic pathway, cellular insults lead to mitochondrial alteration and cytochrome c release. In the presence of cytochrome c and dATP or

ATP, the adaptor protein Apaf-1 assembles into an oligomeric structure known as the apoptosome, which recruits and activates caspase-9 (Li et al., 1997; Zou et al., 1997). Caspase-8, -9, and -10 then activate effector caspases such as caspase-3 and -7, which cleave a wide range of substrates to execute apoptosis.

Caspases are synthesized as single-chain procaspases, which undergo intrachain cleavage to generate the large and small subunits. The molecular requirements for caspases to be catalytically active have been revealed by previous elegant structural studies on active and inactive caspases (Chai et al., 2001; Riedl et al., 2001; Wei et al., 2000). First, a caspase needs to be dimeric to be active because regions from both its own chain and the neighboring chain form the caspase active sites. Specifically, these regions include the L1 and L2 loops of the large subunit and the L3 and L4 loops of the small subunit of one chain and the L2' loop of the small subunit of the neighboring chain. Second, intrachain cleavage facilitates formation of the active site because the L2 and L2' loops are released upon cleavage to become part of the loop bundle that supports the active site. This intrachain cleavage may also stabilize dimerization of some caspases (Boatright et al., 2003; Donepudi et al., 2003). The requirement for cleavage differs among caspases in a manner that appears to depend on the length of the L2-L2' linker region.

Because effector caspases are constitutive dimers, their activation is strictly a consequence of intrachain cleavage by initiator caspases. In contrast to effector caspase activation, intrachain cleavage does not appear to be the crucial factor for initiator caspase activation (Boatright et al., 2003; Donepudi et al., 2003; Srinivasula et al., 2001; Stennicke et al., 1999). For example, caspase-9 can be activated without proteolytic processing. Processed caspase-9 alone is not much more active than procaspase-9. A small population of dimerized uncleavable caspase-8 is as active as processed caspase-8.

An induced proximity model for initiator caspase activation was initially proposed from observations that initiator caspases fused to heterologous dimerizing partners underwent processing and induced cell death (MacCorkle et al., 1998; Muzio et al., 1998; Srinivasula et al., 1998; Yang et al., 1998a; Yang et al., 1998b). This model is consistent with the presence of prodomains in initiator caspases that participate in the assembly of oligomeric complexes in an apoptotic signal dependent fashion. In this model, the pro form of an initiator caspase has low activity that is sufficient for autocatalytic processing when brought into close proximity in these complexes. More recent biochemical studies have led to a revised proximity-induced dimerization model for initiator caspase activation, because caspase-8 and -9 are not constitutive dimers in solution, and specific homodimerization appears to be crucial for their activation (Boatright et al., 2003; Donepudi et al., 2003; Renatus et al., 2001).

For caspase-9, its activity is increased dramatically ($\sim 10^3$ fold) upon association with the apoptosome, and the apoptosome bound caspase-9 is the caspase-9

*Correspondence: haowu@med.cornell.edu

⁵Present address: Department of Therapeutic Proteins, Center for Drug Evaluation and Research, Food and Drug Administration, Bethesda, Maryland 20892.

holoenzyme (C9Holo) (Jiang and Wang, 2000; Rodriguez and Lazebnik, 1999; Srinivasula et al., 2001). Based on the proximity-induced dimerization model, the function of the apoptosome is to promote homodimerization of caspase-9 and, therefore, its activation. In the context of the cryo-EM structure of the heptameric apoptosome, this homodimerization could occur among caspase-9 chains bound on the apoptosome, or the apoptosome bound caspase-9 may dimerize with additional caspase-9 monomers from the solution (Acehan et al., 2002; Shi, 2004; Yu et al., 2005).

Although dimerization does enhance caspase-9 activity, it is not known whether dimerization is sufficient for caspase-9 activation. To address this question, a dimeric form of caspase-9 needs to be constructed, and its activity needs to be quantitatively compared with C9Holo. In an effort to answer this question, a constitutive caspase-9 dimer was engineered by replacing the dimerization residues of caspase-9 with those from caspase-3 (Chao et al., 2005). This engineered caspase-9 dimer is more active than caspase-9 but much less active than C9Holo. Therefore, it was argued that dimerization of caspase-9 is not sufficient for its activation (Chao et al., 2005).

Because replacing residues at the dimerization interface may have compromised the catalytic activity of the engineered caspase-9 dimer, we took an alternative approach to address whether dimerization is sufficient for caspase-9 activation. We replaced the pro domain of caspase-9 (caspase recruitment domain, CARD) with the leucine-zipper dimerization domain of GCN4 (Hu et al., 1990) to promote caspase-9 homodimerization through its intrinsic weak dimerization interface (LZ-C9). We surprisingly found that LZ-C9 is not less active but more active than C9Holo in cleaving the tetrapeptide substrate LEHD-AFC. The measured K_m values of LZ-C9 and C9Holo for LEHD-AFC are similar. The lower activity of C9Holo against LEHD-AFC may be attributed to incomplete C9Holo assembly. This establishes that dimerization is sufficient for catalytic activation of caspase-9. In contrast, LZ-C9 activity for procaspase-3, the physiological substrate of caspase-9, is much lower than C9Holo. This inverse activity of LZ-C9 and C9Holo for LEHD-AFC and procaspase-3 is entirely unexpected. It is not due to feedback cleavage of caspase-9 by caspase-3 or promotion of processed caspase-3 activity by C9Holo. Instead, K_m determination reveals that the K_m of C9Holo for procaspase-3 is much lower than that of LZ-C9, suggesting that apoptosome activates caspase-9 by enhancing its affinity to procaspase-3. This affinity enhancement is important for efficient procaspase-3 activation at the low physiological concentration and makes C9Holo a specific and optimal procaspase-3 processing machine. Collectively, these studies provide unforeseen insights into the molecular basis of caspase-9 activation by the apoptosome.

Results

Engineering of LZ-C9, a Dimeric Caspase-9

To determine whether caspase-9 dimerization is sufficient for its activation, we removed the CARD of procaspase-9 and replaced it with the leucine-zipper dimerization domain of the transcription factor GCN4. A six

residue linker was added in between the leucine zipper and the beginning of the catalytic domain of caspase-9 (LZ-C9, residues 151–416, Figure 1A). In the crystal structure of dimeric CARD-deleted caspase-9 (Renatus et al., 2001), residues L151 at the beginning of the two large subunits in the caspase-9 dimer reside at the same surface of the molecule with a $C\alpha$ distance of 21 Å. In the crystal structure of the GCN4 leucine zipper, the last two residues are disordered, and the distance between the last ordered residue and its symmetry mate is 13 Å (O'Shea et al., 1991). A minimal distance of 4 Å is required to bridge each end of the parallel leucine zipper to L151 of caspase-9. Because the two disordered leucine-zipper residues and a linker of six residues could stretch to approximately 30 Å, the LZ-C9 construct should be sufficient to allow intrinsic caspase-9 dimerization to occur without any constraints, as also shown in a molecular model of LZ-C9 we constructed (Figure 1B).

The calculated molecular weight of LZ-C9 is 34.7 kDa. It elutes as a single peak at 14.6 ml in a Superdex 200 HR 10/300 gel filtration column, suggesting that it is a dimer (Figure 1C). Higher-order oligomerization was not observed. In contrast, CARD deleted caspase-9 (C9 Δ CARD) with a calculated molecular weight of 32.7 kDa elutes at 15.5 ml in the same gel filtration column, which is consistent with the monomeric state of caspase-9. Since gel filtration column elution positions may be influenced by both mass and shape, we used static multiangle light scattering (MALS) in conjunction with refractive index measurements to determine the molecular mass of intact LZ-C9. Consistent with the gel filtration data, MALS measurements gave a molecular mass of 67.6 kDa (0.7% fitting error) with a polydispersity of 1.000, confirming the dimeric state of LZ-C9 (Figure 1D). In contrast, MALS analysis showed that C9 Δ CARD is a monomer with a measured molecular mass of 35.6 kDa (0.7% fitting error) and a polydispersity of 1.000.

LZ-C9 Is More Active than C9Holo for the Tetrapeptide Substrate LEHD-AFC but Much Less Active than C9Holo for the Physiological Substrate Procaspase-3

We used the fluorogenic peptide substrate LEHD-AFC, which is an optimal peptide substrate for caspase-9 (Thornberry et al., 1997), to compare the activity of LZ-C9 with C9Holo. Because intrachain cleavage does not play a significant role in caspase-9 activation, both caspase-9 and LZ-C9 we used are the processed forms. Unexpectedly, at the same caspase-9 concentrations, LZ-C9 gave a significantly faster rate of substrate cleavage than C9Holo (Figure 2A).

Because the physiological substrate of caspase-9 is procaspase-3, we measured the activity of LZ-C9 and C9Holo for procaspase-3 activation. An indirect fluorogenic assay was used in which cleavage of the caspase-3 substrate DEVD-AMC by caspase-9-activated caspase-3 was measured. In contrast to the higher activity of LZ-C9 for the LEHD-AFC peptide substrate, C9Holo is much more efficient in activating procaspase-3 than LZ-C9 (Figure 2B).

Since there are approximately 50 additional residues between the CARD and the beginning of the catalytic domain, we also constructed a longer LZ-C9 construct that includes this additional region (LZ-C9L, residues

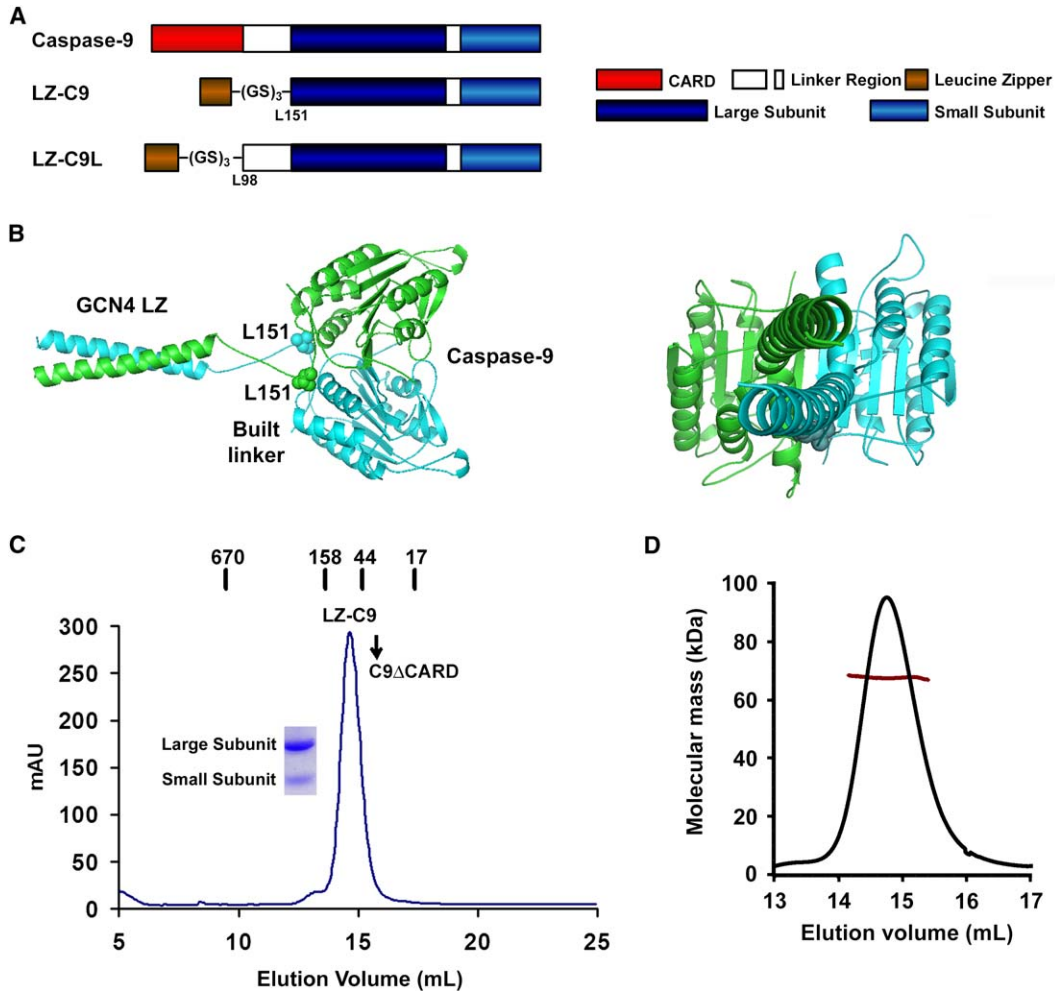


Figure 1. Engineering of LZ-C9, a Dimeric Caspase-9

(A) Schematic diagram of caspase-9, LZ-C9, and LZ-C9L.

(B) A molecular model of LZ-C9 shown as a ribbon diagram. L151 residues of dimeric caspase-9 are shown as space-filling models. Two orientations are shown, left panel with the 2-fold axis horizontal and right panel with the 2-fold axis into the page.

(C) Gel filtration profile of LZ-C9. Locations of molecular weight standards and C9 Δ CARD are marked. SDS-PAGE of the peak fraction is shown.

(D) MALS of LZ-C9. The trace in black corresponds to light-scattering signals at 90°. The trace in dark red shows the variation in molecular mass determination as a function of peak position or elution volume.

98–416). MALS analysis showed that LZ-C9L, with a calculated molecular weight of 40.3 kDa, is also a dimer with a measured molecular mass of 79.1 kDa (2.0% fitting error) and a polydispersity of 1.000. We tested the activity of LZ-C9L against LEHD-AFC and procaspase-3. In comparison with C9Holo, LZ-C9L is more effective in cleaving LEHD-AFC but is much less active against the physiological substrate procaspase-3 (Figure 2C, 2D). Therefore, LZ-C9 (or LZ-C9L) and C9Holo exhibit an inverse capability in cleaving the LEHD-AFC substrate and the physiological substrate procaspase-3.

Feedback Cleavage of Caspase-9 by Caspase-3 Does Not Contribute to the Inverse Activity of LZ-C9 and C9Holo on LEHD-AFC and Procaspase-3

This inverse activity of LZ-C9 and C9Holo for LEHD-AFC and procaspase-3 is intriguing. The human caspase-9 self-mediated intrachain cleavage occurs at Asp 315 (sequence ³¹²PEPD³¹⁵) to generate the large (p35) and small (p12) caspase-9 subunits. However, it has also

been shown that activated caspase-3 can further feedback cleave the N terminus of the small subunit of caspase-9 at Asp330 (sequence ³²⁷DQLD³³⁰) and enhance its activity (Zou et al., 2003). Therefore, we wondered if this feedback cleavage could contribute to the observed difference between C9Holo and LZ-C9 toward the two different substrates.

We mixed the cell pellets of caspase-9 and LZ-C9 with those of nontagged caspase-3 and purified the truncated caspase-9 forms (t-caspase-9 and t-LZ-C9) that have their p12 converted to p10 by the additional cleavage at Asp330. We then repeated the above experiments to determine whether our observations still hold true for these truncated caspase-9 forms (t-C9Holo and t-LZ-C9). Measurement of LEHD-AFC cleavage in the direct fluorogenic assay and procaspase-3 activation in the indirect fluorogenic assay showed that the inverse activity of t-LZ-C9 and t-C9Holo for these substrates is preserved (Figures 2E and 2F). Therefore, caspase-3-mediated cleavage of caspase-9 does not explain this

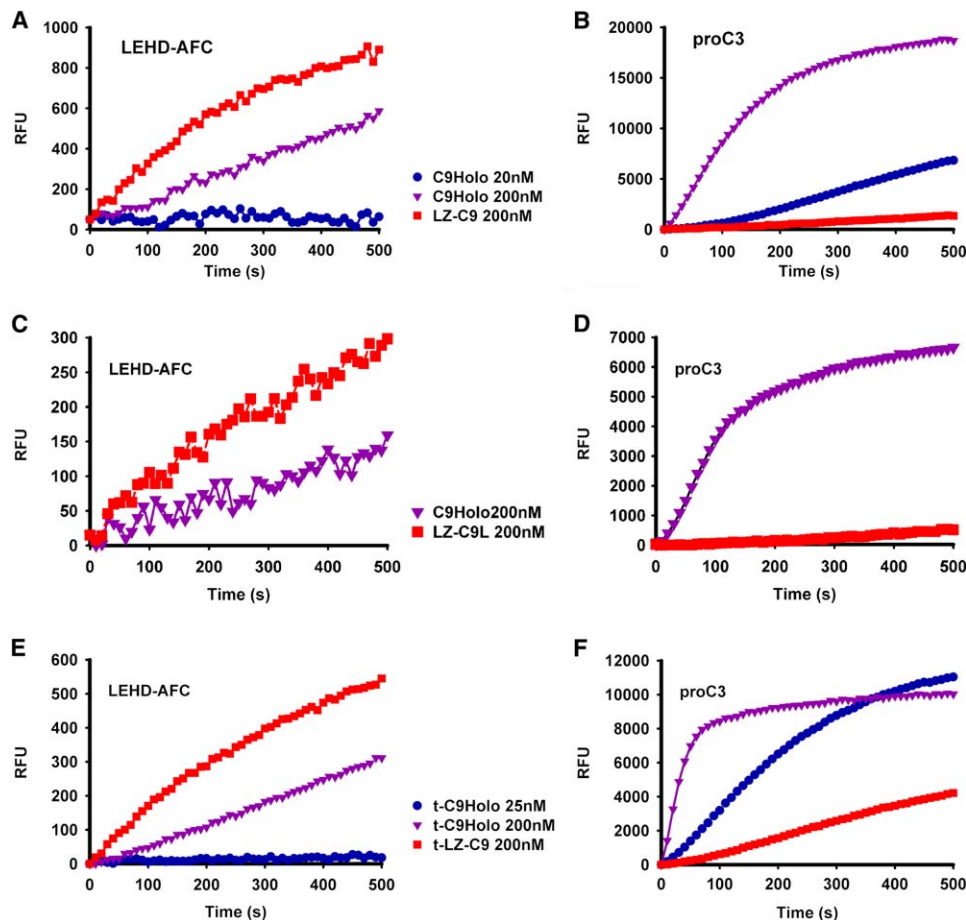


Figure 2. LZ-C9 and C9Holo Have Inverted Activity for LEHD-AFC and Procaspase-3 Substrates

(A, C, and E) Reaction progress curves of tetrapeptide substrate LEHD-AFC cleavage by LZ-C9, LZ-C9L, or t-LZ-C9, respectively, and C9Holo at indicated concentrations. (B, D, and F) Reaction progress curves of DEVD-AMC cleavage by caspase-3 activated by LZ-C9, LZ-C9L, or t-LZ-C9, respectively, and C9Holo at the same concentrations as in (A), (C), and (E).

discrepancy in capability between LZ-C9 and C9Holo for LEHD-AFC and procaspase-3.

Association of Processed Caspase-3 with C9Holo Does Not Increase Caspase-3 Activity

We then examined whether the high efficiency of procaspase-3 activation by C9Holo is due to potential promotion of processed caspase-3 catalytic activity, making C9Holo-processed caspase-3 a caspase-3 holoenzyme. To determine this, we first examined whether caspase-3 can stay associated with C9Holo after processing. We mixed Apaf-1, cytochrome c, dATP, full-length caspase-9, and excess procaspase-3 and subjected the mixture to gel filtration chromatography. All procaspase-3 was cleaved. Indeed, some processed caspase-3 was associated with C9Holo in the early elution fractions (Figure 3A).

We then measured the DEVD-AMC cleavage activities of caspase-3 that was either coeluted with C9Holo or eluted alone to determine whether C9Holo-associated caspase-3 exhibits higher activity. The experiment showed that similar protein levels of caspase-3 in either fraction gave similar catalytic activities (Figure 3B, compare fractions 4 and 9). Serial dilution of a high-concentration caspase-3 fraction to match the caspase-3 level

in the C9Holo fraction confirmed the same observation (Figure 3C, compare fraction 4 with 4-fold- and 8-fold-diluted fraction 12). Similar experiments replacing C9Holo with LZ-C9 showed the absence of caspase-3 protein or activity in the early elution fractions (Figure 3D). These experiments demonstrate that C9Holo-associated caspase-3 does not exhibit higher catalytic activity to cause the observed difference in LZ-C9 and C9Holo against LEHD-AFC and procaspase-3.

LZ-C9 and C9Holo Have Similar K_m Values for LEHD-AFC, and Dimerization Is Sufficient for Catalytic Activation of Caspase-9

To further characterize the catalytic parameters of LZ-C9 and C9Holo, we measured the initial rates of substrate cleavage at different concentrations of LEHD-AFC, from which the K_m values of LZ-C9 and C9Holo for the peptide substrate were determined. The K_m values of LZ-C9 and C9Holo for LEHD-AFC are similar, $465.7 \pm 118.4 \mu\text{M}$ and $686.2 \pm 136.9 \mu\text{M}$, respectively (Figures 4A–4D, Table 1). The K_m values for the feedback-cleaved t-LZ-C9 and t-C9Holo are $260.0 \pm 22.84 \mu\text{M}$ and $276.5 \pm 65.48 \mu\text{M}$, respectively (Figures 4E–4H, Table 1). They are high in comparison with the K_m values of other caspases for their peptide substrates (Zhou et al., 1998).

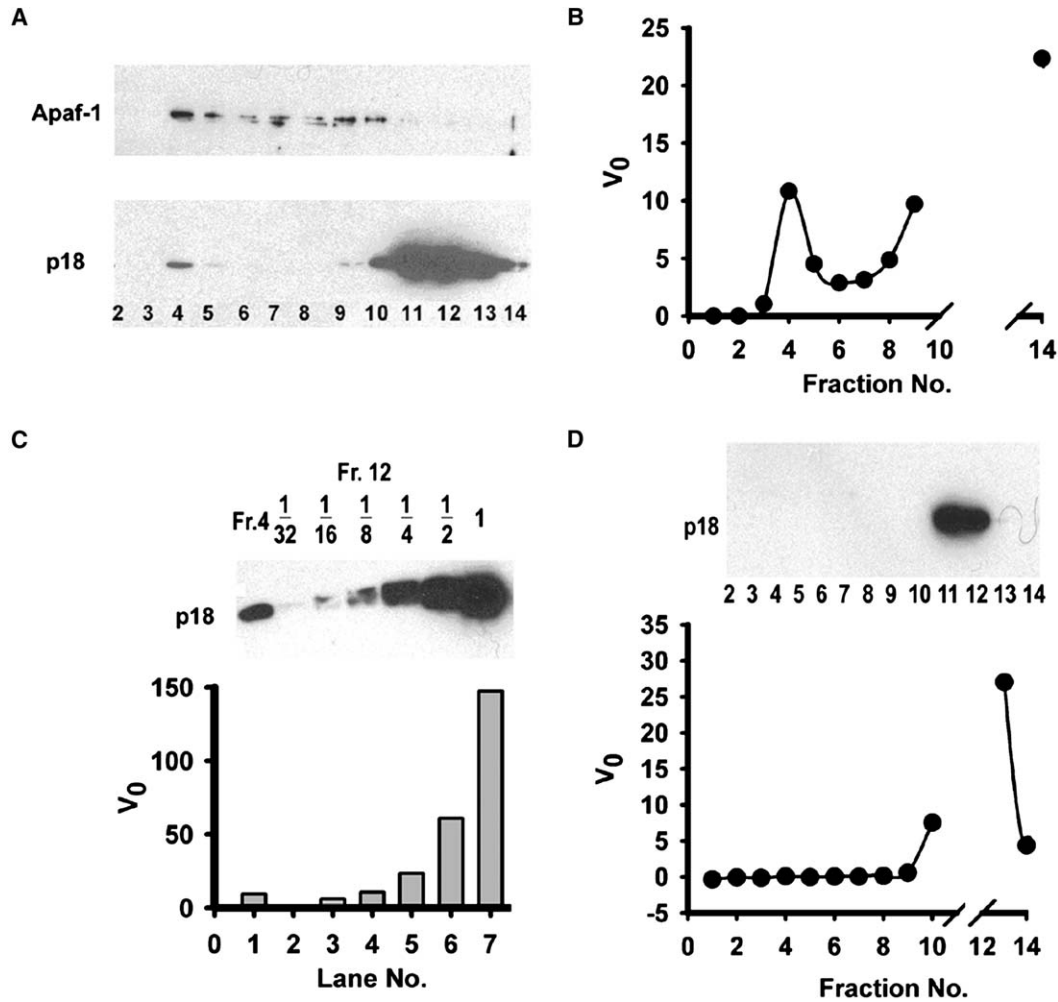


Figure 3. Association of C9Holo with Processed Caspase-3 Does Not Enhance Caspase-3 Activity
 (A) Excess procaspase-3 was incubated with C9Holo, and the mixture was subjected to gel filtration. Aliquots of fractions were resolved by 15% SDS-PAGE followed by Western blotting using antibodies against Apaf-1 (upper panel) and caspase-3 (lower panel).
 (B) Fractions were also assayed for their cleavage activity against DEVD-AMC. The initial velocities were plotted as a function of fraction numbers. Activities of fractions 10–13 were too high for initial velocities to be determined precisely, and they were not shown.
 (C) Fraction 12 was serially diluted in 2-fold steps. Aliquots of each dilution were analyzed by 15% SDS-PAGE along with an aliquot of fraction 4 and blotted against caspase-3 (upper panel). They were also assayed for cleavage activity against DEVD-AMC. The initial velocities were plotted (lower panel).
 (D) Excess procaspase-3 was incubated with LZ-C9 under the same conditions as in (A), and the mixture was subjected to gel filtration. Fractions were resolved by 15% SDS-PAGE and blotted against caspase-3 (upper panel). Aliquots of fractions were assayed for cleavage activity against DEVD-AMC. The initial velocities were plotted as a function of fraction numbers (lower panel). Activities of fractions 11 and 12 were too high for initial velocities to be determined precisely, and they were not shown.

Since caspase-9 and Apaf-1 need to be assembled into the large multimeric caspase-9 holoenzyme for caspase-9 activation, we asked whether the observed lower activity of C9Holo for LEHD-AFC is due to incomplete apoptosome and C9Holo assembly and hence lower effective concentration of C9Holo. Alternatively, a lower intrinsic turnover rate, k_{cat} , of C9Holo, can also contribute to the observed lower activity. To distinguish these two possibilities, we titrated excess Apaf-1 into caspase-9 to facilitate assembly of C9Holo. This titration increased the rate of LEHD-AFC cleavage when caspase-9 concentration remained constant (Figure 4). At the highest Apaf-1 concentration we could provide, the activity of C9Holo did not catch up with the activity of LZ-C9. These data suggest that holoenzyme assembly is a limiting

factor contributing to the lower activity of C9Holo to the LEHD-AFC substrate. The data also suggest that the observed striking difference between C9Holo and LZ-C9 in activating procaspase-3 (Figure 2B) is still an underestimation because of incomplete holoenzyme assembly. On the other hand, it is likely that the catalytic activities of C9Holo and LZ-C9, exemplified in K_m and k_{cat} for LEHD-AFC, are equivalent. Thus, dimerization appears to be sufficient for catalytic activation of caspase-9.

C9Holo Has Dramatically Higher Substrate Affinity for Procaspase-3 than LZ-C9

Why, then, does C9Holo activate caspase-3 much more efficiently than LZ-C9? Is it possible that C9Holo

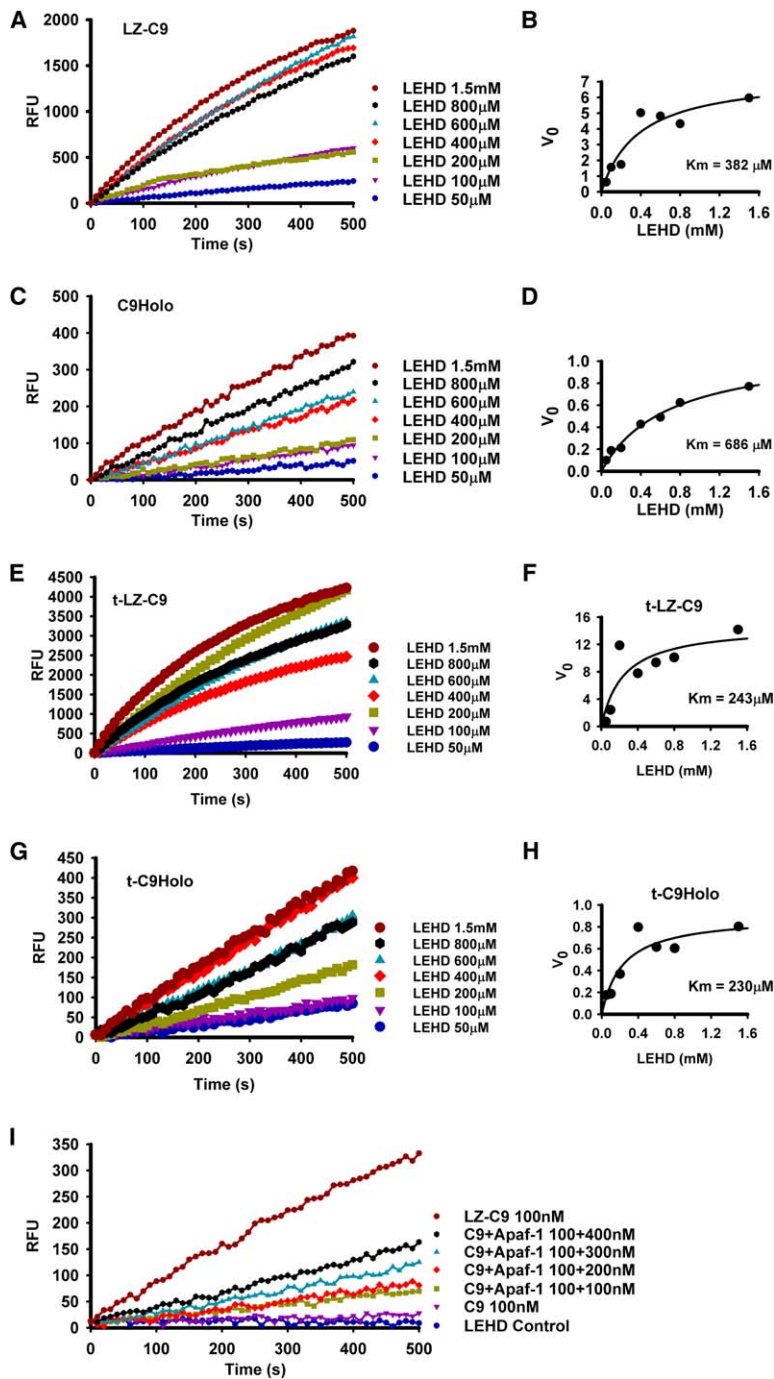


Figure 4. LZ-C9 and C9Holo Have Similar K_m Values for Tetrapeptide Substrate LEHD-AFC (A, C, E, and G) Reaction progress curves of LEHD-AFC cleavage at different concentrations by LZ-C9 (100 nM), C9Holo (100 nM full-length caspase-9, 100 nM Apaf-1, 10 μ M dATP, and 500 nM cytochrome c), t-LZ-C9 (100 nM), and t-C9Holo (100 nM full-length truncated caspase-9, 100 nM Apaf-1, 10 μ M dATP, and 500 nM cytochrome c), respectively. (B, D, F, and H) Plots of initial velocities as a function of LEHD-AFC concentrations for LZ-C9, C9Holo, t-LZ-C9, and t-C9Holo, respectively. (I) Reaction progress curves of LEHD-AFC cleavage by caspase-9 at different Apaf-1 concentrations.

possesses a higher affinity for procaspase-3 than LZ-C9? To examine this, we measured the rates of substrate cleavage at different concentrations of procaspase-3 to determine the K_m values of C9Holo and LZ-C9 for procaspase-3. We used the indirect fluorogenic assay, in which cleavage of the caspase-3 substrate DEVD-AMC was measured. The slope of the DEVD-AMC cleavage at a given time point is indicative of the active caspase-3 concentration at that time point and was used to derive K_m values for the procaspase-3 cleavage reaction. Surprisingly, the K_m of C9Holo for procaspase-3 is 139.3 ± 23.19 nM (Figures 5A and 5B, Table 1), about three orders of magnitude lower than that for LEHD-AFC. In contrast,

the K_m of LZ-C9 for procaspase-3 was estimated to be much higher; at the highest possible concentration of procaspase-3 we could supply, the reaction did not show any sign of saturation (Figures 5C and 5D). This difference in K_m values between C9Holo and LZ-C9 is also exemplified in the much higher effect of increasing procaspase-3 concentration on the ability of LZ-C9 than on the ability of C9Holo to activate procaspase-3 (Figures 5A and 5C).

Similarly, we showed that the K_m value of t-C9Holo for procaspase-3 is 79.8 ± 18.5 nM (Figures 5E and 5F, Table 1), similar to its nontruncated counterpart. These data demonstrate that both C9Holo and t-C9Holo have

Table 1. Measured K_m Values of C9Holo, t-C9Holo, LZ-C9, and t-LZ-C9 for LEHD-AFC and Procaspase-3

	K_m for LEHD-AFC	K_m for Procaspase-3
C9Holo	686.2 ± 136.9 μM^a	Average 139.3 ± 23.19 nM ^{b,d} (1) 155.7 ± 86.2 nM ^a (2) 122.9 ± 28.1 nM ^a
t-C9Holo	Average 276.5 ± 65.48 $\mu\text{M}^{b,c}$ (1) 230.2 ± 76.2 μM^a (2) 322.8 ± 250.2 μM^a	79.8 ± 18.5 nM ^a
LZ-C9	Average 465.7 ± 118.4 $\mu\text{M}^{b,d}$ (1) 382 ± 185.1 μM^a (2) 549.4 ± 231.8 μM^a	High ^e
t-LZ-C9	Average 260.0 ± 22.84 $\mu\text{M}^{b,c}$ (1) 243.8 ± 194.7 μM^a (2) 276.1 ± 240.3 μM^a	High ^e

^a The errors in individual K_m measurements represent the scatter of the data points from the hyperbolic fittings.

^b When two measurements are available, the average K_m values are shown along with the individual measurements. The errors in average K_m values are standard deviations from the two measurements.

^c One protein preparation was used in the two individual measurements for obtaining the average K_m values.

^d Two different protein preparations were used in the two individual measurements for obtaining the average K_m values.

^e K_m values could not be determined from the current data.

high affinity to procaspase-3. Therefore, we show unexpectedly that one important mechanism of caspase-9 activation by the apoptosome is by enhancing its affinity to the physiological substrate procaspase-3.

Discussion

Dimerization Is Sufficient for Catalytic Activation of Caspase-9

Caspase-9 is unusual in that it is only active when bound to the apoptosome. Such activation is so dramatic that the apoptosome bound caspase-9 is known as the caspase-9 holoenzyme (Rodriguez and Lazebnik, 1999; Srinivasula et al., 2001). Other caspases, including caspase-8, an initiator caspase in the extrinsic apoptosis pathway, can directly activate their substrates without the requirement to be bound to an accelerator. Our data on the catalytic properties of LZ-C9 and C9Holo show that caspase-9 dimerized by a leucine zipper is not less active but more active than the caspase-9 holoenzyme. This demonstrates that dimerization is sufficient for catalytic activation of caspase-9.

The measured K_m values of caspase-9 holoenzyme and LZ-C9 for LEHD-AFC are similar. They are also similar to the previously reported K_m values of caspase-9 for LEHD-AFC (Renatus et al., 2001; Zou et al., 2003). How about the intrinsic turnover rate of caspase-9 holoenzyme in comparison with LZ-C9? The similar K_m but lower activity of the caspase-9 holoenzyme could indicate that it possesses a lower k_{cat} than LZ-C9 for LEHD-AFC. However, because the apoptosome might also mediate caspase-9 dimerization, it is unlikely that its k_{cat} is lower than that of leucine-zipper-dimerized caspase-9. Since caspase-9 holoenzyme requires assembly, a more plausible explanation to the lower activity is that the effective concentration of C9Holo is lower than its apparent concentration. This is supported by the increase of activity upon titration of more Apaf-1. There-

fore, we conclude that the catalytic activity of LZ-C9 is equivalent to that of caspase-9 holoenzyme for peptide substrate LEHD-AFC.

Our data contradict the observation from an engineered dimeric caspase-9 made by replacing the weak dimerization residues of caspase-9 with the strong dimerization residues of caspase-3 (Chao et al., 2005). The difference may be that LZ-C9 likely promotes dimerization through its intrinsic dimerization interface, while the altered dimerization interface in the engineered dimer may have affected its catalytic ability, even against LEHD-AFC.

Enhanced Affinity of C9Holo for Procaspase-3 Is Important for Efficient Procaspase-3 Activation at the Physiological Concentration

Although dimerization appears to be sufficient for establishing the catalytic competency of caspase-9, it is not sufficient for the high efficiency of caspase-9 holoenzyme to support procaspase-3 activation, because LZ-C9 is much less efficient in procaspase-3 activation. Our data indicate that procaspase-3 is a much better substrate for the caspase-9 holoenzyme with dramatically increased affinity. Therefore, apoptosome activates caspase-9 by both dimerization and enhanced affinity to its physiological substrate, procaspase-3.

This affinity enhancement is important if the endogenous concentration of procaspase-3 in cells is low—for example, around the K_m of C9Holo—but much below the K_m of LZ-C9. Indeed, previous reports have shown this to be the case. Using quantitative Western analysis, the approximate concentration of procaspase-3 in 293 cells was found to be around 100 nM (Stennicke et al., 1998), which is similar to the K_m of C9Holo for procaspase-3. Independently, caspase-3 concentration in Jurkat T cells was estimated to be below 100 nM (Pop et al., 2001; Saunders et al., 2000). At this procaspase-3 concentration, only C9Holo, but not dimerized caspase-9, can efficiently cleave procaspase-3 substrate. The small yet likely significant reduction in the K_m of C9Holo for procaspase-3 by the feedback cleavage of caspase-9 (Table 1) may further enhance the ability of C9Holo to process procaspase-3 at the physiological concentration.

C9Holo Is a Specific Procaspase-3 Processing Machine

In the intrinsic apoptosis pathway, C9Holo appears to have a strict specificity for procaspase-3 and its relative procaspase-7. Other caspase-9 substrates have not been reported. This situation differs from the initiator caspase in the extrinsic apoptosis pathway, caspase-8, which cleaves procaspase-3 as well as BID, a BH3-only Bcl-2 family member (Li et al., 1998; Luo et al., 1998).

This strict specificity may be conferred by association of caspase-9 with the apoptosome in the form of C9Holo. In contrast, caspase-8 gets released upon activation from the DISC (Peter and Krammer, 2003). The intrinsic substrate specificity of caspase-9, as determined by its specificity for four-residue peptide sequences, is not stricter than caspase-8 or any other caspases (Thornberry et al., 1997). However, because the K_m of caspase-9 or C9Holo for these peptides are unusually high, caspase-9 is essentially inactive against potential

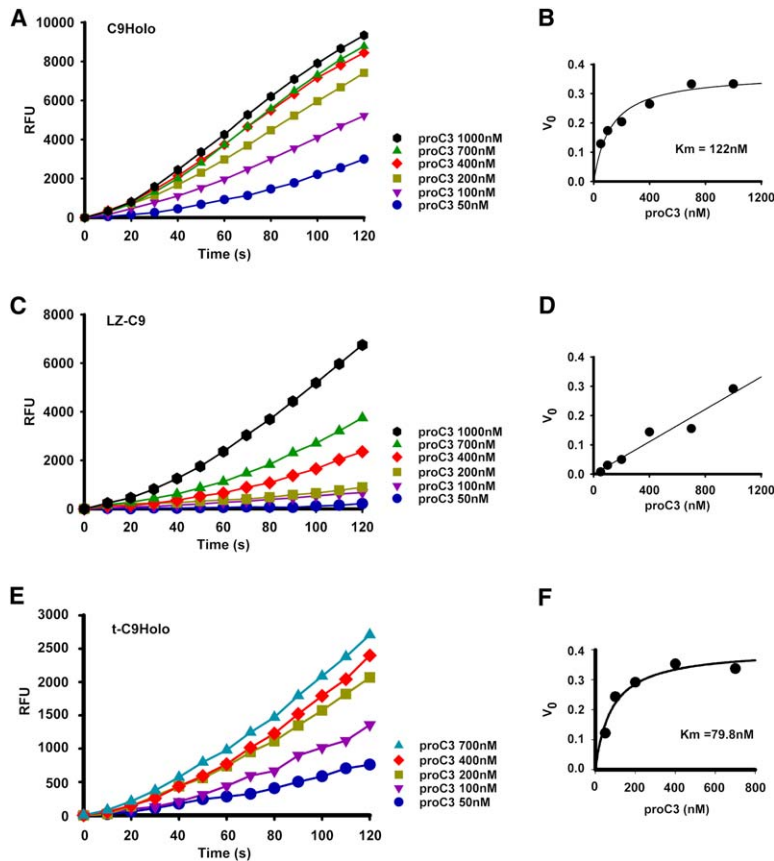


Figure 5. C9Holo Has Much-Reduced K_m for Procaspase-3

(A, C, and E) Reaction progress curves of procaspase-3 activation at different procaspase-3 concentrations by C9Holo (25 nM), LZ-C9 (200 nM), and t-C9Holo (25 nM), respectively. These were measured indirectly by the cleavage of the caspase-3 substrate DEVD-AMC. (B, D, and F) Plots of initial velocities as a function of procaspase-3 concentrations for C9Holo, LZ-C9, and t-C9Holo, respectively.

substrates. Only in the form of C9Holo, caspase-9 has an enhanced affinity specifically for procaspase-3, which makes C9Holo a specific processing machine for procaspase-3. Therefore, in addition to providing higher affinity for procaspase-3, association of caspase-9 with the apoptosome might also ensure its specificity for procaspase-3.

Potential Molecular Mechanisms of Affinity Enhancement of C9Holo for Procaspase-3

So what are the possible mechanisms for the enhanced affinity of caspase-9 holoenzyme for procaspase-3? First, the apoptosome may directly interact with procaspase-3 and therefore enhance the affinity of bound caspase-9 to procaspase-3 (Figure 6A). In this model, the apoptosome plays a direct contact role in procaspase-3 recruitment. Alternatively, the apoptosome may induce conformational changes in bound caspase-9 and therefore increase its affinity to procaspase-3 (Figure 6B). The conformational changes may possibly lie outside the immediate active site, as it does not affect the cleavage of LEHD-AFC.

It is also possible that this enhanced affinity may be due to avidity by a simultaneous recognition of two cleavage sites from two adjacent caspase-9 dimers (Figure 6C). The rationale is that, in the platform of the oligomeric apoptosome, C9Holo may simultaneously interact with both cleavage sites on procaspase-3, leading to enhanced affinity via avidity. In contrast, LZ-C9, with its single productive active site (Chao et al., 2005; Renatus et al., 2001), cannot gain affinity through this avidity. We have tried to test this hypothesis by linking two active

site mutant (C163A) of procaspase-3 sequences in tandem via a flexible covalent linker (1-277-[GS]₇-1-277). This single-chain procaspase-3-C163A construct harbors the entire heterotetrameric sequence of procaspase-3 and contains two caspase-9 cleavage sites. We then mutated the second caspase-9 cleavage site in this single chain procaspase-3 construct (D175A) to generate a procaspase-3 dimer with a single caspase-9 recognition sequence. However, the cleavage activities of C9Holo against the single chain wild-type or D175 mutant did not show dramatic differences (data not shown). It is possible that the lack of dramatic differences may also be due to the incomplete destruction of the second caspase-9 recognition site by the single D175A mutation. A more stringent test on this hypothesis is to generate monomeric procaspase-3. But previous (Bose and Clark, 2001) as well as our own experiments (data not shown) have indicated that monomeric procaspase-3 mutant cannot be generated without greatly altering the structure of procaspase-3. Therefore, it remains to be seen whether the potential concerted recognition of two cleavage sites by C9Holo contributes to this high affinity.

Regardless of the exact mechanism, it is clear that C9Holo has dramatically increased affinity to procaspase-3 and therefore exhibits dramatically increased activity and specificity for this physiological substrate. This characteristic places caspase-9 as a single unique caspase in the entire caspase superfamily in that it defies the otherwise universal activation mechanism of cleavage and/or dimerization. While dimerization of caspase-9 transforms it into an active enzyme when using its

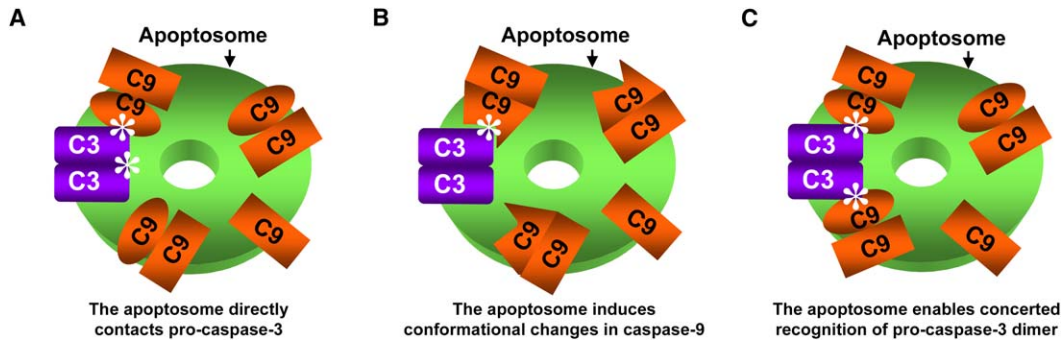


Figure 6. Potential Molecular Mechanisms of Affinity Enhancement of C9Holo for Procaspase-3

The apoptosome, caspase-9 (C9), and procaspase-3 (C3) are shown in green, orange, and purple, respectively. The inactive caspase-9 subunits are shown as rectangles. Asterisks denote contacts of procaspase-3 with either the apoptosome or caspase-9. For simplicity, only one procaspase-3 dimer is shown.

optimal peptide as the substrate, the K_m of the enzyme for the substrate is high ($\sim 10^{-3}$ – 10^{-4} M) compared to those of other caspases ($\sim 10^{-4}$ – 10^{-5} M) (Zhou et al., 1998). Therefore, caspase-9 requires the additional step of activation, the association into C9Holo, to be fully activated for processing its physiological substrate at the low physiological concentration (~ 100 nM), ensuring a precise and versatile regulation. In summary, our quantitative characterization of C9Holo and LZ-C9 provided unexpected insights into the molecular mechanism of caspase-9 activation by the apoptosome and adds to our understandings of caspase activation in general.

Experimental Procedures

Protein Expression and Purification

His-tagged full-length human caspase-9, leucine-zipper caspase-9 (LZ-C9 and LZ-C9L), and CARD-deleted caspase-9 (C9 Δ CARD, residues 139–416) were expressed in *E. coli*. LZ-C9 contains the initiation Met, leucine-zipper sequence from GCN4 (251–281), a linker (GSGSGS), and the C-terminally His-tagged catalytic domain of human caspase-9 (151–416). LZ-C9L is similar to LZ-C9 except that it includes the additional region between the CARD and the catalytic domain of caspase-9 (98–416). Both LZ-C9 and LZ-C9L were purified by Ni-NTA affinity chromatography (Qiagen), anion exchange at pH 8.0 with HiTrap Q (GE Healthcare) and gel filtration chromatography with Superdex 200 HR 10/300 (GE Healthcare). The buffer for gel filtration contains 20 mM Tris (pH 7.5), 150 mM NaCl, and 5 mM DTT. To generate caspase-3 feedback-cleaved full-length caspase-9 and LZ-C9, their respective cell pellets were mixed with those of non-tagged caspase-3 and purified similarly. His-tagged Apaf-1 and procaspase-3 were expressed in the baculovirus-mediated insect cell expression system. They were purified by Ni-NTA affinity chromatography followed by gel filtration. Caspase concentrations were determined by both the Bradford assay and active site titration as described previously (Stennicke and Salvesen, 2000; Zou et al., 2003), which agree well with each other.

Modeling of LZ-C9

A molecular model of LZ-C9 was constructed using the GCN4 leucine-zipper coordinates (PDB ID 2ZTA) and caspase-9 coordinates (PDB ID 2AR9). The eight residue linker comprising the two disordered residues in GCN4 and the GSGSGS sequence was built from an eight residue loop in PDB ID 1Z3G containing a similar sequence. Model building was done in O (Jones et al., 1991), and the ribbon diagram was produced in PyMOL (DeLano Scientific).

Caspase Activity Assay

C9Holo and LZ-C9 activities were monitored by turnover of fluorogenic tetrapeptide substrates in both direct and indirect assays. Fluorescence measurement upon substrate cleavage was per-

formed on SpectraMax M2 plate reader (Molecular Devices) using 384-well plates (Corning). All measurements were performed in 20 μ l reactions in buffer A (20 mM HEPES [pH 7.5], 10 mM KCl, 1.5 mM MgCl₂, 1 mM EDTA, 1 mM EGTA, and 1 mM DTT) at 37°C. Reaction mixtures also contain 10 μ M dATP (Sigma) and 500 nM bovine heart cytochrome c (1 μ M if Apaf-1 concentration is higher than 200 nM, Sigma) when measuring C9Holo activity. In direct assay, C9Holo or LZC9 of indicated concentration was incubated at 37°C for 5 min. The reactions were initiated by adding the substrate Ac-LEHD-AFC (100 μ M, Calbiochem). Release of the AFC moiety was monitored at emission wavelength of 505 nm with the excitation wavelength of 400 nm. In indirect assay, C9Holo or LZ-C9 was incubated together with Ac-DEVD-AMC (15 μ M) at 37°C for 5 min before procaspase-3 was added to initiate the reactions. The reactions were then followed at emission wavelength of 465 nm with excitation wavelength of 360 nm. Reactions were monitored at 10 s intervals. V_0 was drawn from the initial phase of the progress curve. K_m values were determined using nonlinear regression method to fit Michaelis-Menton equation.

MALS

Molar mass of purified LZ-C9, LZ-C9L and C9 Δ CARD was determined by static MALS. Protein was injected onto a Superdex 200 HR 10/300 gel filtration column equilibrated in a buffer containing 20 mM Tris (pH 7.5), 150 mM NaCl, and 0.2 mM DTT. The chromatography system was coupled to a three-angle light scattering detector (mini-DAWN EOS) and refractive index detector (Optilab DSP) (Wyatt Technology). Data were collected every 0.5 s at a flow rate of 0.2 ml/min. Data analysis was carried out using the program ASTRA, yielding the molar mass and mass distribution (polydispersity) of the sample.

Fractionation of Procaspase-3 and Apoptosome Mixture

Excess procaspase-3 (2 μ M) was incubated with 1 μ M Apaf-1, 2 μ M cytochrome c, 10 μ M dATP, and 1 μ M caspase-9 at 30°C for 30 min in a total volume of 600 μ L. Reaction mixture was then fractionated on a Superdex 200 column preequilibrated with buffer A at 4°C. The column was eluted with buffer A, and fractions of 1 ml were collected. Aliquots of 2 μ l of each fraction were assayed for their cleavage activity against DEVD-AMC as described. Aliquots of 10 μ l of each fraction were resolved by 15% SDS-PAGE followed by Western blot analysis (see below). Alternatively, excess procaspase-3 was incubated with 1 μ M LZ-C9 for 30 min at 30°C. The mixture underwent the same fractionation and analyses as described above.

Western Blot Analysis

Proteins were transferred from SDS-PAGE gel to PVDF membrane using Trans-Blot SD (Bio-Rad). After transfer, membrane was probed with either mouse monoclonal anti-caspase-3 (Cell Signaling) (1:1000) or polyclonal anti-Apaf-1 (1:1000). Washed blot was then incubated with horseradish peroxidase-conjugated horse anti-mouse (caspase-3) or goat anti-rabbit (Apaf-1) IgG. Reactive bands were visualized using SuperSignal West Pico Kit (Pierce) as instructed.

Acknowledgments

The work was supported by the National Institute of Health (R01 AI-50872). S.-C.L. and Y.-C.L. are Cancer Research Institute postdoctoral fellows.

Received: December 11, 2005

Revised: February 27, 2006

Accepted: March 30, 2006

Published: April 20, 2006

References

- Acehan, D., Jiang, X., Morgan, D.G., Heuser, J.E., Wang, X., and Akey, C.W. (2002). Three-dimensional structure of the apoptosome: implications for assembly, procaspase-9 binding, and activation. *Mol. Cell* 9, 423–432.
- Boatright, K.M., Renatus, M., Scott, F.L., Sperandio, S., Shin, H., Pedersen, I.M., Ricci, J.E., Edris, W.A., Sutherlin, D.P., Green, D.R., and Salvesen, G.S. (2003). A unified model for apical caspase activation. *Mol. Cell* 11, 529–541.
- Bose, K., and Clark, A.C. (2001). Dimeric procaspase-3 unfolds via a four-state equilibrium process. *Biochemistry* 40, 14236–14242.
- Chai, J., Wu, Q., Shiozaki, E., Srinivasula, S.M., Alnemri, E.S., and Shi, Y. (2001). Crystal structure of a procaspase-7 zymogen: mechanisms of activation and substrate binding. *Cell* 107, 399–407.
- Chao, Y., Shiozaki, E.N., Srinivasula, S.M., Rigotti, D.J., Fairman, R., and Shi, Y. (2005). Engineering a dimeric caspase-9: a re-evaluation of the induced proximity model for caspase activation. *PLoS Biol.* 3, e183. 10.1371/journal.pbio.0030183.
- Daniel, N.N., and Korsmeyer, S.J. (2004). Cell death: critical control points. *Cell* 116, 205–219.
- Donepudi, M., Mac Sweeney, A., Briand, C., and Grutter, M.G. (2003). Insights into the regulatory mechanism for caspase-8 activation. *Mol. Cell* 11, 543–549.
- Hu, J.C., O'Shea, E.K., Kim, P.S., and Sauer, R.T. (1990). Sequence requirements for coiled-coils: analysis with lambda repressor-GCN4 leucine zipper fusions. *Science* 250, 1400–1403.
- Jiang, X., and Wang, X. (2000). Cytochrome c promotes caspase-9 activation by inducing nucleotide binding to Apaf-1. *J. Biol. Chem.* 275, 31199–31203.
- Jones, T.A., Zou, J.-Y., Cowan, S.W., and Kjeldgaard, M. (1991). Improved methods for building models in electron density maps and the location of errors in those models. *Acta Crystallogr. A* 47, 110–119.
- Li, P., Nijhawan, D., Budihardjo, I., Srinivasula, S.M., Ahmad, M., Alnemri, E.S., and Wang, X. (1997). Cytochrome c and dATP-dependent formation of Apaf-1/caspase-9 complex initiates an apoptotic protease cascade. *Cell* 91, 479–489.
- Li, H., Zhu, H., Xu, C.J., and Yuan, J. (1998). Cleavage of BID by caspase 8 mediates the mitochondrial damage in the Fas pathway of apoptosis. *Cell* 94, 491–501.
- Luo, X., Budihardjo, I., Zou, H., Slaughter, C., and Wang, X. (1998). Bid, a Bcl2 interacting protein, mediates cytochrome c release from mitochondria in response to activation of cell surface death receptors. *Cell* 94, 481–490.
- MacCorkle, R.A., Freeman, K.W., and Spencer, D.M. (1998). Synthetic activation of caspases: artificial death switches. *Proc. Natl. Acad. Sci. USA* 95, 3655–3660.
- Muzio, M., Stockwell, B.R., Stennicke, H.R., Salvesen, G.S., and Dixit, V.M. (1998). An induced proximity model for caspase-8 activation. *J. Biol. Chem.* 273, 2926–2930.
- O'Shea, E.K., Klemm, J.D., Kim, P.S., and Alber, T. (1991). X-ray structure of the GCN4 leucine zipper, a two-stranded, parallel coiled coil. *Science* 254, 539–544.
- Peter, M.E., and Krammer, P.H. (2003). The CD95(APO-1/Fas) DISC and beyond. *Cell Death Differ.* 10, 26–35.
- Pop, C., Chen, Y.R., Smith, B., Bose, K., Bobay, B., Tripathy, A., Franzen, S., and Clark, A.C. (2001). Removal of the pro-domain does not affect the conformation of the procaspase-3 dimer. *Biochemistry* 40, 14224–14235.
- Renatus, M., Stennicke, H.R., Scott, F.L., Liddington, R.C., and Salvesen, G.S. (2001). Dimer formation drives the activation of the cell death protease caspase 9. *Proc. Natl. Acad. Sci. USA* 98, 14250–14255.
- Riedl, S.J., and Shi, Y. (2004). Molecular mechanisms of caspase regulation during apoptosis. *Nat. Rev. Mol. Cell Biol.* 5, 897–907.
- Riedl, S.J., Fuentes-Prior, P., Renatus, M., Kairies, N., Krapp, S., Huber, R., Salvesen, G.S., and Bode, W. (2001). Structural basis for the activation of human procaspase-7. *Proc. Natl. Acad. Sci. USA* 98, 14790–14795.
- Rodriguez, J., and Lazebnik, Y. (1999). Caspase-9 and APAF-1 form an active holoenzyme. *Genes Dev.* 13, 3179–3184.
- Salvesen, G.S. (2002). Caspases and apoptosis. *Essays Biochem.* 38, 9–19.
- Saunders, P.A., Cooper, J.A., Roodell, M.M., Schroeder, D.A., Borchert, C.J., Isaacson, A.L., Schendel, M.J., Godfrey, K.G., Cahill, D.R., Walz, A.M., et al. (2000). Quantification of active caspase 3 in apoptotic cells. *Anal. Biochem.* 284, 114–124.
- Shi, Y. (2002). Mechanisms of caspase activation and inhibition during apoptosis. *Mol. Cell* 9, 459–470.
- Shi, Y. (2004). Caspase activation: revisiting the induced proximity model. *Cell* 117, 855–858.
- Srinivasula, S.M., Ahmad, M., Fernandes-Alnemri, T., and Alnemri, E.S. (1998). Autoactivation of procaspase-9 by Apaf-1-mediated oligomerization. *Mol. Cell* 1, 949–957.
- Srinivasula, S.M., Hegde, R., Saleh, A., Datta, P., Shiozaki, E., Chai, J., Lee, R.A., Robbins, P.D., Fernandes-Alnemri, T., Shi, Y., and Alnemri, E.S. (2001). A conserved XIAP-interaction motif in caspase-9 and Smac/DIABLO regulates caspase activity and apoptosis. *Nature* 410, 112–116.
- Stennicke, H.R., and Salvesen, G.S. (2000). Caspase assays. *Methods Enzymol.* 322, 91–100.
- Stennicke, H.R., Jurgensmeier, J.M., Shin, H., Deveraux, Q., Wolf, B.B., Yang, X., Zhou, Q., Ellerby, H.M., Ellerby, L.M., Bredesen, D., et al. (1998). Pro-caspase-3 is a major physiologic target of caspase-8. *J. Biol. Chem.* 273, 27084–27090.
- Stennicke, H.R., Deveraux, Q.L., Humke, E.W., Reed, J.C., Dixit, V.M., and Salvesen, G.S. (1999). Caspase-9 can be activated without proteolytic processing. *J. Biol. Chem.* 274, 8359–8362.
- Thornberry, N.A., Rano, T.A., Peterson, E.P., Rasper, D.M., Timkey, T., Garcia-Calvo, M., Houtzager, V.M., Nordstrom, P.A., Roy, S., Vailancourt, J.P., et al. (1997). A combinatorial approach defines specificities of members of the caspase family and granzyme B. Functional relationships established for key mediators of apoptosis. *J. Biol. Chem.* 272, 17907–17911.
- Wei, Y., Fox, T., Chambers, S.P., Sintchak, J., Coll, J.T., Golec, J.M., Swenson, L., Wilson, K.P., and Charifson, P.S. (2000). The structures of caspases-1, -3, -7 and -8 reveal the basis for substrate and inhibitor selectivity. *Chem. Biol.* 7, 423–432.
- Yang, X., Chang, H.Y., and Baltimore, D. (1998a). Autoproteolytic activation of pro-caspases by oligomerization. *Mol. Cell* 1, 319–325.
- Yang, X., Chang, H.Y., and Baltimore, D. (1998b). Essential role of CED-4 oligomerization in CED-3 activation and apoptosis. *Science* 281, 1355–1357.
- Yu, X., Acehan, D., Menetret, J.F., Booth, C.R., Ludtke, S.J., Riedl, S.J., Shi, Y., Wang, X., and Akey, C.W. (2005). A structure of the human apoptosome at 12.8 Å resolution provides insights into this cell death platform. *Structure* 13, 1725–1735.
- Zhou, Q., Krebs, J.F., Snipas, S.J., Price, A., Alnemri, E.S., Tomaselli, K.J., and Salvesen, G.S. (1998). Interaction of the baculovirus anti-apoptotic protein p35 with caspases. Specificity, kinetics, and characterization of the caspase/p35 complex. *Biochemistry* 37, 10757–10765.
- Zou, H., Henzel, W.J., Liu, X., Lutschg, A., and Wang, X. (1997). Apaf-1, a human protein homologous to C. elegans CED-4, participates in cytochrome c-dependent activation of caspase-3. *Cell* 90, 405–413.
- Zou, H., Yang, R., Hao, J., Wang, J., Sun, C., Fesik, S.W., Wu, J.C., Tomaselli, K.J., and Armstrong, R.C. (2003). Regulation of the Apaf-1/caspase-9 apoptosome by caspase-3 and XIAP. *J. Biol. Chem.* 278, 8091–8098.